LONG, MEDIUM AND SHORT RANGE ORDER CHANGES IN AMORPHOUS SiO_2 EXPOSED TO ALKALI SILICA REACTION

A. Hamoudi[1], L. Khouchaf[1,*], P. Cordier[2]

[1] Centre de Recherche de l'Ecole des Mines de Douai, 941 rue Charles Bourseuil BP. 10838 59508 DOUAI, France

[2] Laboratoire de Structure et Propriétés de l'Etat Solide, UMR 8008 USTL UFR de Physique Bat C6 59655 VILLENEUVE D'ASCQ CEDEX, France.

Abstract

Long, medium and short order changes induced by alkali silica reaction of amorphous SiO_2 compounds were performed using controlled pressure scanning electron microscope (CP-SEM), x-ray diffraction (XRD), x-ray absorption near edge structure (XANES), and nuclear magnetic resonance ^{29}Si NMR-MAS. Micro absorption experiments have been carried out using x-ray micro beam from a synchrotron radiation source with high brightness. Our study using synthetic amorphous SiO_2 as the starting material leads to the same results obtained in the natural alkali-silica gels. The reactivity of amorphous SiO_2 compounds induces mainly the formation of Q3 species and alkalis-rich domains. The structure of SiO_2 was affected and the correlation between structural changes and some parameters characterizing the reactivity of SiO_2 was done. Micro XANES spectra show the presence of different environments of silicon: one with four oxygen atoms and the other with a number of oxygen lower than four in agreement with previous studies.

Keywords: SiO_2 reactivity, SEM, XRD, XANES, NMR

1 INTRODUCTION

The alkali silica reaction (ASR) is a deleterious chemical process that occurs between amorphous or poorly crystallized SiO_2, present in the mineral aggregates of concrete, and the alkali and hydroxyl ions in the aqueous solution inside the concrete pores. The durability of concrete is severely affected by the alkali silica reaction. Many studies were performed in order to explain the mechanisms involved in the ASR [1,2]. They have shown that the efficiency of the ASR is strongly dependent on the micro structural state of the starting material. As an illustration, the reactivity of synthetic alpha quartz, with less structural disorder and impurities is very low [3,4,5]. The quartz is thermodynamically more stable than the silica polymorphs tridymite, cristobalite and moganite. Polymorphs react more than quartz under ASR process [4]. Previous studies on the ASR in the natural flint [5,6,7] have shown that the reaction begins with the breaking of bridge siloxane Si-O-Si and formation of amorphous and nanocrystalline phase. However the presence in the flints of different structural areas, such as crystallized, poorly-crystallized and amorphous domains makes the study of the mechanism of degradation and the kinetics of the reaction more complex. Thus, we used the amorphous silica model as a starting material in order to obtain information about the mechanism that is established during the responsiveness of the amorphous part in the natural flint aggregate submitted to ASR.

2 MATERIALS AND METHODS

2.1 Starting material

The starting material used in this study is a synthetic amorphous silica powder from Alpha Aesar with high purity (99.9%). SiO_2 has been checked by X-ray fluorescence analysis and the average grain size showed two maxima, at 3 μm and 22 μm. a-SiO2 is used here to indicate amorphous silica with a glassy, non-crystalline structure, as opposed to crystalline <alpha>-SiO2 (alpha-silica).

Amorphous silica has been submitted to ASR through a procedure which has been previously described [8]. 1g of silica powder introduced in a closed stainless steel container with a mixture of 0.5 g of portlandite $Ca(OH)_2$. After 30 minutes of preheating 10 ml of potash solution KOH at 0.79

* Corresponding author: *khouchaf@ensm-douai.fr*
Tel: +33-3-27-71-23-19

mol/L were added slowly to the mixed powder in a large beaker over a magnetic stirrer to produce a homogeneous slurry and then autoclaved in an oven to develop ASR at 80°C for 312 hours. After a reaction period, depolymerisation of silica gives new products studied below.

2.2 Methods

Controlled Pressure Scanning electron microscope (CP-SEM)

Observations (range order μm-nm) were carried out at accelerating voltage of 15 kV and a probe current of 130 pA using a FEG controlled pressure scanning electron microscope (CP-SEM) "Hitachi S4300 SE/N" equipped with EDS ultra dry thermo with silicon drift detector (SDD). Observations were performed under vacuum pressure of 0.37 Torr. Low pressure gas (air) is introduced inside the analysis chamber in order to avoid coating operation. The influence of the interaction between electron beam and gas on imaging and microanalysis results was controlled carefully [6,9,10]. EDS analyses were performed with internal standards and the LLDs is 0.1wt%.

X-ray powder diffraction (XRD)

XRD (range order 50-100□) spectra were recorded for 2θ values between 10° and 100° with steps of 0.007° and a counting time of 10s per step using a Bruker D8 Advance diffractometer operating at 40kV and 40 mA with Co radiation (λ ≈ 1.78897Å). No specific preparation has been performed before experiment. The original powder has been introduced in Al_2O_3 cup which was maintained under rotation during experiment.

X-ray absorption near edge structure (XANES)

Micro XANES (range order ≤20 Å) experiments were carried out on the LUCIA beam line at the Swiss light source (SLS). The high brightness of synchrotron radiation leads to obtain data with good quality from micro zones of heterogeneous materials. Micro XANES spectra at Si K-edge, were recorded using InSb(111) monochromators. Spectra were recorded, at room temperature, under high vacuum (10^{-5} Torr) in total electron yield (TEY) mode on a grain embedded in epoxy resin. Micro-zones have been studied with 6x12 μm^2 beam sizes.

^{29}Si magic-angle spinning (MAS) NMR

^{29}Si MAS NMR (range order ≤5 Å) spectra were recorded at room temperature using a Brucker Avance 100 NMR spectrometer with field of 2.34 Tesla. ^{29} Si MAS experiments operating at 19.89 MHz were performed with a 7mm MAS probe with ZrO2 rotor at a spinning rate of 4 kHz. Tetra methyl silane (TMS) was used as a reference for chemical shifts measurements. Spectra were recorded with a pulse angle of π/5 and a recycle delay of 80s, which enable relaxation. The number of scans was 256 for each sample.

3 RESULTS

Figure 1a shows an image obtained by CP-SEM using back scatter imaging of a grain of silica after the reaction. A second micrograph (Figure 1b) shows random oriented needles of nanometre size (~ 100 nm). In order to visualize the distribution of different cations within the silica, element maps have been made using EDS (Figure 2). They show a heterogeneous aspect of the attack. X-ray elemental maps of silicon Si, calcium Ca, and potassium K show that Ca and K are present in all parts of the grain.

Figure 3 shows diffractograms of silica submitted to ASR, compared with pristine amorphous silica for reference. The reference sample (a) exhibits a broad peak typical for amorphous silica [11] with a maximum located at 25 °2θ. Several changes are observed in the diffractograms of reacted silica (b). The diffractogram is completely different, revealing structural changes at long range order (ie.50-100□). Strong reflections emerge, indicating the presence of new crystalline phases.

Using a micro beam (6X12 μm^2) delivered by synchrotron radiation facility, absorption spectra at Si K edge at different zones of the grain (from the inside to outside) absorption experiments were performed. Figure 4 exhibits XANES spectra of the attacked silica at different points of the grain compared to amorphous silica in Total Electron Yield mode. All spectra present a peak at 1846.8 eV. However, a second peak around 1843 eV appears only in the degraded silica. The intensity of this peak increases from the inside towards the outside of the grain.

The MAS solid-state ^{29}Si NMR spectrum of the starting silica (Figure 4a) exhibits a signal centred at -110 ppm, attributed unambiguously to Q_4 units in the amorphous silica [12]. The width of this resonance indicates a broad distribution of Si-O-Si angles, which is synonymous with a disordered structure. These lines can be identified according to literature data with the different tetrahedral Q_n

environments of Si in silicates [13], according to standard Q_n nomenclature denoting the connectivity of silicate tetrahedron, with n the number of associated bridging oxygens (Si-O-Si).

When reaction proceeds (Figure 4b), additional resonances appear at -90, -85 and -79 ppm and attributed to Q_3, Q_2 and Q_1 units, respectively [13,14], while the Q_4 peak attributed to amorphous silica has completely disappeared.

4 DISCUSSION

In a recent study [15], we have shown that the heterogeneity of the aggregate plays an important role in the mechanism of the reaction. At the beginning of the reaction we have shown that, only potassium diffuses inside the grain while the calcium remains outside the grain. In the present work, the penetration of Ca and K in all parts of the grain indicates that the portlandite $Ca(OH)_2$ is totally consumed by the ASR, this was confirmed by XRD. The ratio C/S was quantified by microanalysis X, we found that it is less than 0.6 for this sample depending on the zone analyzed. The total consumption of portlandite by the reaction involves the formation of stable phases in our samples. This makes more pertinent information obtained with analysis of the local order.

XRD results show the occurrence of a range of poorly crystalline compounds. The majority of these reflections were attributed to a calcium silicate hydrate (C-S-H). The C-S-H compounds are highly complex, and with widely varying composition. The peaks largely match the ICDD card file numbers 83-1520, 34-0002, and 06-0453. C-S-H morphology is illustrated in Figure 2b, showing disordered needles of nanometere size (~ 100 nm). The identification was made by comparing our spectra with those found in the literature [16,17].

The broad peak located at 25 °2θ in our reference samples has lost most intensity which leads us to assume that the amorphous starting silica SiO_2 network had almost disappeared during the reaction. No traces of portlandite phase were detected showing that all the portlandite is consumed by the reaction. This is interesting for our study in short and medium scale because the product of the reaction analyzed consists of stable phases.

In order to obtain information about the medium range order (≤20 Å), we carried out an experiment by X-ray absorption near edge structure (XANES). This analytical technique, unlike X-ray diffraction, can be used both for crystalline and amorphous materials and gives information on medium-range order. It has been established that the various energy resonances above the edge are a signature of the presence of environment with a different degree of coordination for silicon atoms [7,18,19]. XANES spectra of the attacked silica at different points of the grain compared to amorphous silica. All spectra present a peak at 1846.8 eV, which is associated with the electronic transitions of the 1s to 3p state and attributed to tetrahedral environment around the silicon [7]. However, a second peak around 1843 eV appears in the degraded silica only. The intensity of this peak increases from the inside to outside of the grain. At present, the origin of this peak may be explained by the presence of silicon atoms surrounded by a number of oxygen lower than four [20,21].

Because the reaction affects the Si-O-Si bonds [5,15] complementary information about the evolution of the short-range order (≤5 Å), around silicon atoms is obtained from ^{29}Si NMR. Several broad peaks can be observed, typical of a distribution of isotopic chemical shift values caused by structural disorder. The reaction induces depolymerisation of the SiO_2 framework, creating Q_3 species similar to the sheet silicate structure, Q_2 species (SiO_4 tetrahedra within silicate chains) and Q_1 (tetrahedra at the end of silicate chain).

5 CONCLUSIONS

SEM, XRD, XANES, and NMR were used to follow long, medium and short range order of amorphous silica submitted to alkali-silica reaction. The results allowed us to identify the calcium silicates hydrate phases formed after the reaction, and showed that portlandite is totally consumed by the reaction after this attack time. SiO_2 tetrahedrons, which form the structure of our starting silica are most affected following the attack by the ASR. These results are confirmed by XANES and NMR analysis. Micro XANES spectra show the presence of different environments of silicon with either four oxygen atoms or with a number of oxygen lower than four. NMR results show that the predominantly Q_4 species present in the starting amorphous SiO_2 depolymerisation give way to principally Q_3 and Q_2. More investigations are under consideration in order to correlate with extended X-ray absorption fine structure (EXAFS) results.

6 ACKNOWLEDGMENTS

X-ray absorption experiments were performed at the Swiss Light Source, Paul Scherrer Institut, Villigen, Switzerland. It was approved by the advisory committee. The authors thank the EC for financial support and Dr A.M. Flank for his help with the synchrotron radiation experiments.

7 REFERENCES

[1] Chatterji, S, and Thaulow, N (2000): Some fundamental aspect of alkali-silica reaction. In: Bérubé, MA, Fournier, B, and Durand, B (editors): Proceedings of the 11th International Conference on Alkali-Aggregate Reaction in Concrete, Quebec, Canada: 21.

[2] Dent Glasser LS, and Kataoka, N (1981): The chemistry of alkali-aggregate reaction. Proceedings of the 5th International Conference on Alkali-Aggregate Reaction in Concrete, Cape Town (South Africa). National Building Research Institute of CSIR: 7.

[3] Verstraete, J (2005): Approche multi-technique et multi-echelle d'etude des proprietes structurales des materiaux heterogenes: application a un granulat siliceux naturel. PhD thesis, Université de Haute Alsace, France: pp 217

[4] Broekmans, MATM (2004): The quality of quartz and its susceptibility for ASR. Materials Characterization (53/2- 4), Special Issue (29): 129-140.

[5] Khouchaf, L, and Verstraete, J (2007): Multi-technique and multi-scale approach applied to study the structural behavior of heterogeneous materials: natural SiO_2 case. Journal of Materials Science (42): 2455-2462.

[6] Khouchaf, L, and Boinski, F (2007): Environmental scanning electron microscope study of SiO_2 heterogeneous material with helium and water vapor. Vacuum (81): 599-603.

[7] Khouchaf, L, Verstraete, J, Prado, RJ, and Tuilier, M, H (2005): XANES, EXAFS and RMN contributions to follow the structural evolution induced by alkali-silica reaction in SiO_2 aggregate. Physica Scripta (T115): 552-555.

[8] Verstraete, J, Khouchaf, L, Flank, AM, and Tuilier, MH (2004): Amorphisation mechanism of a flint aggregate during the alkali-silica reaction: X-ray diffraction and X-ray absorption XANES contributions. Cement & Concrete Research (34): 581-586.

[9] Khouchaf, L, and Verstraete, J (2002): X-ray microanalysis in the Environment scanning electron microscope (ESEM): small size particles analysis limits. Journal de Physique IV (112): 341-346.

[10] Khouchaf, L, and Verstraete, J (2004): Electron scattering by gas in the environmental scanning electron microscope (ESEM): effects on the image quality and on the X-ray microanalysis. Journal de Physique IV (118): 237-243.

[11] Tambelli, CE, Schneider, JF, Hasparyk, NP, and Monteiro, PJM (2006): Study of the structure of alkali-silica reaction gel by high-resolution NMR spectroscopy. Journal of Non-Crystalline Solids (352): 3429-3436.

[12] Cong, XD, and Kirkpatrick, RJ (1993): ^{29}Si MAS NMR Spectroscopy Investigation of alkali silica reaction product gels. Cement & Concrete Research (23): 811-823.

[13] Kirkpatrick, RJ (1988): MAS NMR spectroscopy of minerals and glasses. In Hawthorne, FC (editor): Spectroscopic methods in mineralogy and geology. Reviews in Mineralogy (18): 341-403.

[14] Cong, XD, and Kirkpatrick, RJ (1996): ^{29}Si MAS NMR Study of the structure of calcium silicate hydrate. Advanced Cement Based Materials (3): 144-156.

[15] Khouchaf, L, Boinski, F, Tuilier, MH, and Flank, AM (2006): Characterization of heterogeneous SiO_2 materials by scanning electron microscope and micro fluorescence XAS techniques, Nuclear Instruments and Methods in Physics Research B (252): 333-338.

[16] Minet, J (2003): Synthèse et caractérisation de silicates de calcium hydrates hybrids. PhD thesis, Université Paris XI, Orsay : pp 170.

[17] Black, L, Garbev, K, Beuchle, G, Stemmermann, P, and Schild, D (2006): X-ray photoelectron spectroscopic investigation of nanocrystalline calcium silicate hydrates synthesised by reactive milling. Cement & Concrete Research (36): 1023-1031.

[18] Li, D, Bancroft, GM, Kasrai, M, Fleet, ME, Feng, XH, Tan, KH, and Yang, BX (1993): High-resolution Si K- and $L_{2,3}$-edge XANES of α quartz and stishovite. Solid State Communication (87/7): 1613-1617.

[19] Li, D, Bancroft, GM, Kasrai, M, Fleet, ME, Secco, RA, Feng, XH, Tan, KH, and Yang, BX (1994): X-ray absorption spectroscopy of silicon dioxide (SiO_2) polymorphs; the structural characterization of opal. American Mineralogist (79): 622-632.

[20] Belot, V, Corriu, RJP, Leclercq, D, Lefèvre, P, Mutin, PH, Vioux, A, and Flank, AM (1991): Sol-gel route to silicon suboxides Preparation and characterization of silicon sesquioxide. Journal of Non-Crystalline Solids (127): 207-214.

[21] Flank, AM, Karnatak RC, Blancad, C, Esteva, JM, Lagarde, P, and Connerade, JP (1991): Probing matrix isolated SiO molecular clusters by X-ray absorption spectroscopy. Zeitschrift der Physik, Reihe D – Atoms, Molecules and Clusters (21): 357-366.

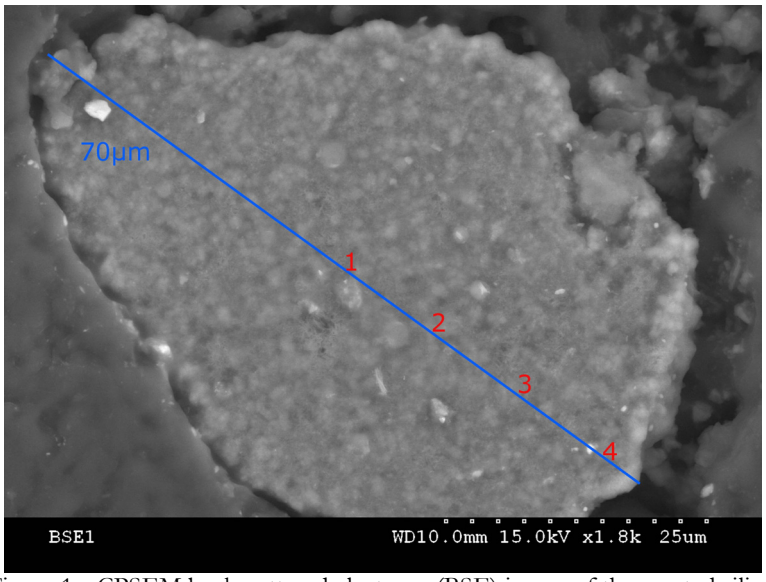

Figure 1a: CPSEM backscattered electrons (BSE) image of the reacted silica.

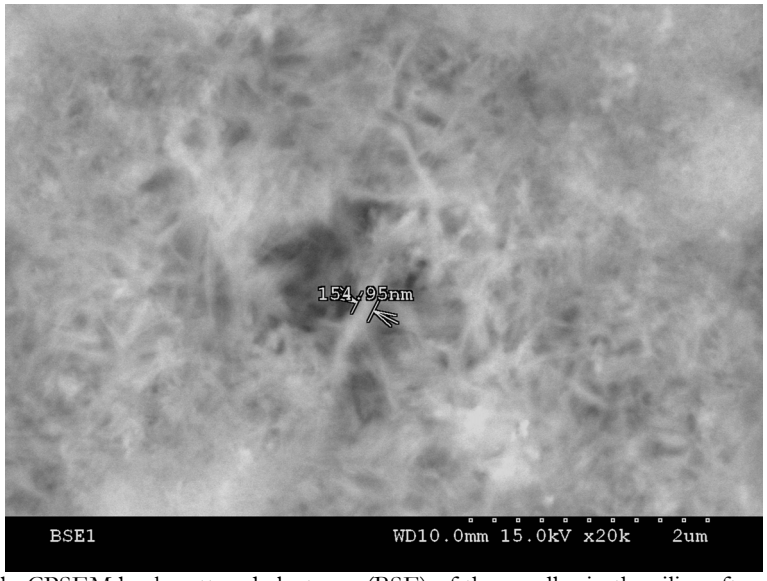

Figure 1b: CPSEM backscattered electrons (BSE) of the needles in the silica after reaction.

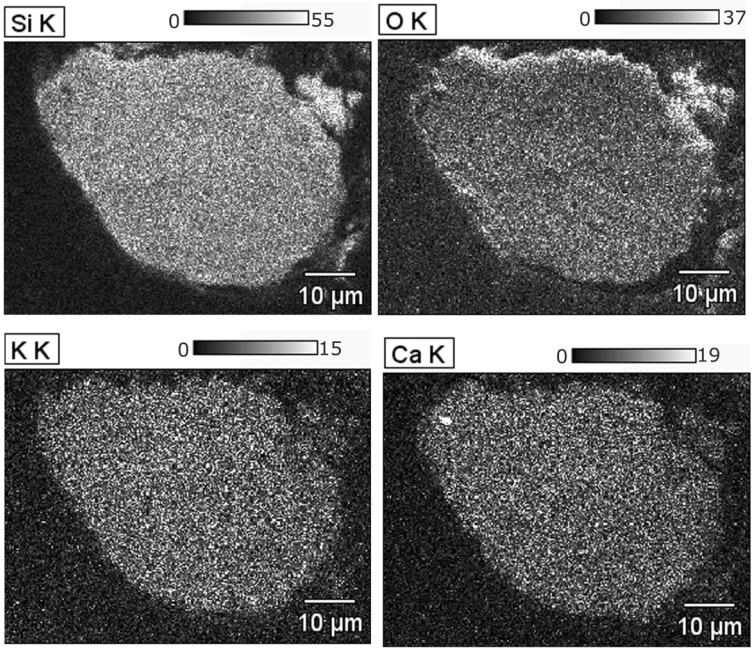

Figure 2: Elemental maps of Si, O, K and Ca.

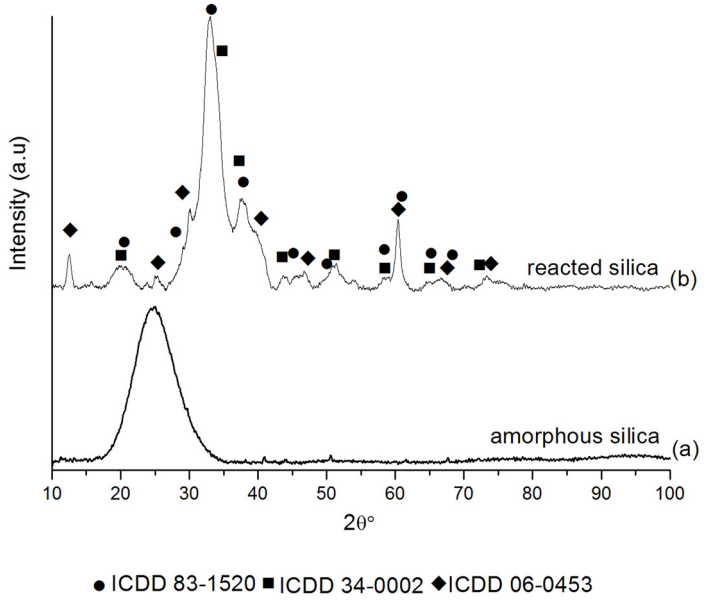

Figure 3: X-ray diffraction spectra of the starting silica (a) and reacted silica (b).

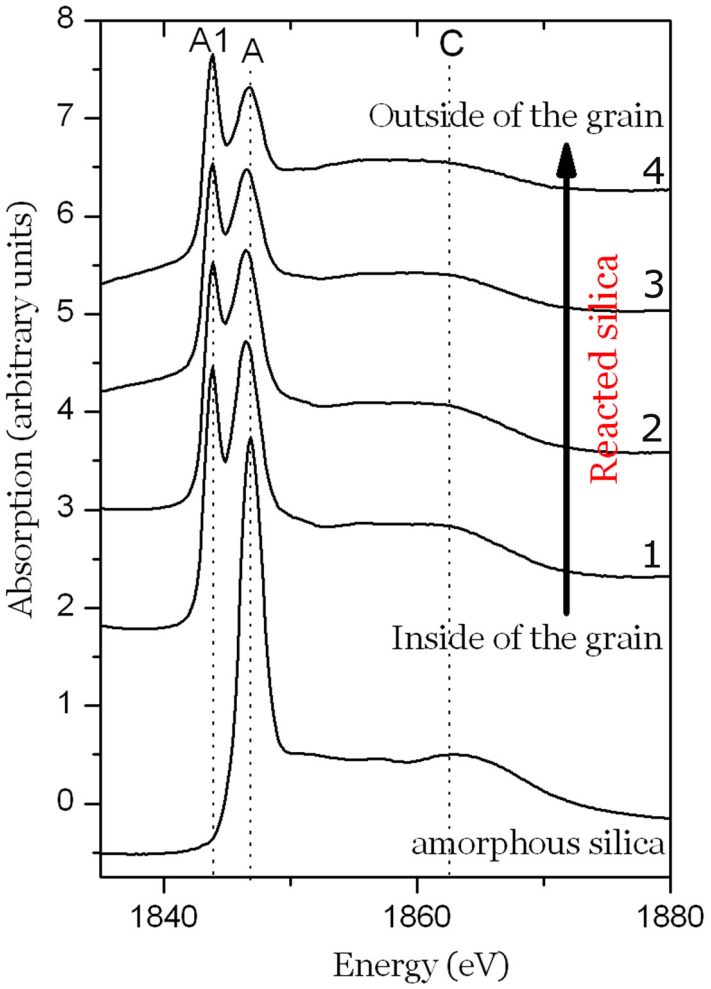

Figure 4: XANES spectra at Si K-edge of the silica reference and the silica submitted to ASR at different zones in the grain.

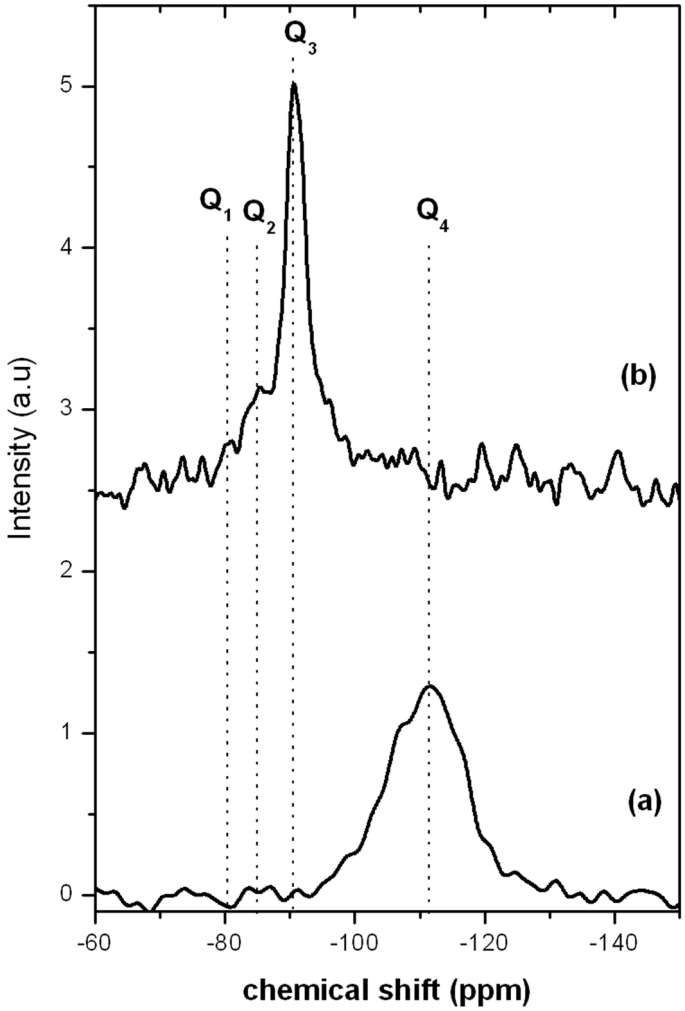

Figure 5: ^{29}Si MAS NMR spectra of silica reference (a) and reacted silica (b).